Sirt5 regulates chondrocyte metabolism and osteoarthritis development through protein lysine malonylation

Huanhuan Liu[1,2], Anupama Binoy[1,2], Siqi Ren[1,2], Thomas C. Martino[1,2], Anna E. Miller[1,2], Craig R. G. Willis[4], Shivakumar R. Veerabhadraiah[5], Abhijit Sukul[1,2], Michael J. Jurynec[5], Shouan Zhu[1,2,3*]

[1]Department of Biomedical Sciences, Heritage College of Osteopathic Medicine (HCOM), Ohio University, Athens, OH, 45701, USA

[2]Ohio Musculoskeletal and Neurological Institute (OMNI), Heritage College of Osteopathic Medicine (HCOM), Ohio University, Athens, OH, 45701, USA

[3]Diabetes Institute (DI), Heritage College of Osteopathic Medicine (HCOM), Ohio University, Athens, OH, 45701, USA

[4]School of Chemistry and Biosciences, Faculty of Life Sciences, University of Bradford, Bradford, BD7 1DP, UK

[5]Department of Orthopaedics, University of Utah, Salt Lake City, Utah, 84108 USA.

[*]Correspondence to

Shouan Zhu: Department of Biomedical Sciences, Ohio Musculoskeletal and Neurological Institute (OMNI), Diabetes Institute (DI), Heritage College of Osteopathic Medicine (HCOM), Ohio University, OH, 45701, USA. zhus1@ohio.edu

Abstract:

Objectives: Chondrocyte metabolic dysfunction plays an important role in osteoarthritis (OA) development during aging and obesity. Protein post-translational modifications (PTMs) have recently emerged as an important regulator of cellular metabolism. We aim to study one type of PTM, lysine malonylation (MaK) and its regulator Sirt5 in OA development.

Methods: Human and mouse cartilage tissues were used to measure SIRT5 and MaK levels. Both systemic and cartilage-specific conditional knockout mouse models were subject to high-fat diet (HFD) treatment to induce obesity and OA. Proteomics analysis was performed in *Sirt5*$^{-/-}$ and WT chondrocytes. SIRT5 mutation was identified in the Utah Population Database (UPDB).

Results: We found that SIRT5 decreases while MAK increases in the cartilage during aging. A combination of Sirt5 deficiency and obesity exacerbates joint degeneration in a sex dependent manner in mice. We further delineate the malonylome in chondrocytes, pinpointing MaK's predominant impact on various metabolic pathways such as carbon metabolism and glycolysis. Lastly, we identified a rare coding mutation in *SIRT5* that dominantly segregates in a family with OA. The mutation results in substitution of an evolutionally invariant phenylalanine (Phe–F) to leucine (Leu–L) (F101L) in the catalytic domain. The mutant protein results in higher MaK level and decreased expression of cartilage ECM genes and upregulation of inflammation associated genes.

Conclusions: We found that Sirt5 mediated MaK is an important regulator of chondrocyte cellular metabolism and dysregulation of Sirt5-MaK could be an important mechanism underlying aging and obesity associated OA development.

INTRODUCTION

Osteoarthritis (OA) is a degenerative joint disease that affects millions of people worldwide (*1*, *2*), with no currently available disease-modifying drugs. One of the central features of OA is gradual loss of articular cartilage. It has been increasingly recognized that chondrocyte metabolic dysfunctions during various OA risk conditions such as aging, obesity, and injury is an important mechanism for cartilage degeneration (*3*). However, it is still unknown how dysregulated cellular metabolism happens and how to correct it for potential therapeutics development.

Protein post-translational modifications (PTMs) are key regulators of cellular functions and metabolic pathways (*4*-*6*). Abnormal accumulation of these PTMs in metabolically active organs, such as the liver, has been found to play an important role in development of obesity and aging-associated diseases. For example, increased acetylation of proteins in the liver that regulate fatty acid oxidation accelerates the development of metabolic syndrome (*7*). We previously reported that there is an abnormal accumulation of protein post-translational malonylation, succinylation, and acetylation at lysine residues in the cartilage of obese mice (*8*). This presumably is due to accumulation of reactive acyl-group metabolic byproducts during obesity such as malonyl-CoA, succinyl-CoA, and acetyl-CoA, a phenomenon termed as 'cellular carbon stress' (*5*). Mammals possess 7 sirtuins (Sirt1-7), several of which have the ability to remove those PTMs (*4*). Sirtuin 5 (Sirt5) is a NAD^+-dependent deacylase that can remove various acyl groups from lysine residues, such as malonyl (*9*), succinyl (*9*), and glutaryl (*10*) groups. Through its demalonylation activity, Sirt5 can modulate the levels of lysine malonylation (MaK), a PTM that has been demonstrated to mainly target glycolysis in the liver and linked to metabolic disorders (*11*). We reasoned that Sirt5-MaK signaling axis could potentially play an important role in chondrocyte functions and OA development, as chondrocytes rely substantially on glycolysis to generate ATP (*12*-*14*). Indeed, we previously discovered that Sirt5 expression declines in chondrocytes during aging, leading to increased MaK and altered glucose metabolism (*15*). Moreover, obesity also increases MaK in chondrocytes, which may further impair their function and contribute to OA development.

In this study, we aimed to explore the age-related changes in SIRT5-MaK signaling and investigate the impact of SIRT5 deficiency in combination with obesity on chondrocyte function and elucidate the molecular mechanisms by which SIRT5 regulates cartilage homeostasis. Additionally, we identified a rare, dominantly inherited SIRT5 mutation ($SIRT5^{F101L}$) in a familial OA cohort and

examined its functional consequences in chondrocytes. Our findings provide new insights into the role of SIRT5 in cartilage metabolism and OA pathogenesis, offering potential avenues for therapeutic intervention in this debilitating disease.

METHODS

Animals and diet experiment

Sirt5 heterozygous knockout mice (*B6;129-Sirt5tm1FWa/J*, Stock No. 012757), *Aggrecan-Cre*^{ERT2} mice (*B6.Cg-Acan*$^{tm1(cre/ERT2)Crm}$*/J*, Stock No. 019148), and *Sirt5*$^{flox/flox}$ mice (*B6.129S(SJL)-Sirt5*$^{tm1.1/cs}$*/AuwJ*, Stock No.033456) were purchased from The Jackson Laboratory. The mice were then bred to generate the genotype required for this study and treated with different diets. Detailed information can be found in the supplementary materials.

Identification of human SIRT5 mutation

We used the Utah Population Database (UPDB) to identify SIRT5 mutation. The detailed diagnostic and procedure codes used to identify individuals with osteoarthritis in the UPDB can be found in the supplementary materials.

RESULTS

Sirt5 decreases while MaK increases in the cartilage during aging

To investigate the impact of aging on MaK and Sirt5 in joint tissues, we conducted immunohistochemical staining of MaK and SIRT5 in human knee articular cartilage samples obtained from donors spanning different age groups. In the young group, a majority of chondrocytes exhibited robust SIRT5 expression, whereas MaK staining was faint. Conversely, in the elderly group, MaK expression was markedly enhanced while SIRT5 staining was notably reduced (Figure 1A). Further quantitative analysis assessed the proportions of chondrocytes strongly stained, weakly stained, or unstained for SIRT5 and MaK relative to total chondrocyte counts. The results indicated a nearly 70% decline in the ratio of strongly SIRT5-stained chondrocytes in older donors compared to younger ones, whereas MaK expression showed an opposite trend (Figure 1B). To corroborate these findings in humans, we examined cartilage tissue

from mice of different ages: young (25 weeks), middle-aged (48 weeks), and old (90 weeks). Consistently, we observed a significant age-associated increase in MaK levels (Figure 1C and 1D).

In summary, our findings suggest that aging is associated with altered expression patterns of MaK and SIRT5 in both human and mouse joint tissues, with MaK levels increasing significantly with age. These results highlight potential age-related changes in metabolic pathways within chondrocytes that merit further investigation.

Sirt5 systemic knockout (*Sirt5*$^{-/-}$) exacerbates HFD induced metabolic dysfunctions and OA development in mice in a sex dependent manner

In our previous work, we highlighted Sirt5 as a critical regulator of chondrocyte cellular metabolism (*15*), noting that *Sirt5*$^{-/-}$ mice exhibit mild spontaneous cartilage degeneration by 10 months of age (*8*). We also demonstrated that another major OA risk factor, obesity, also increases MaK in the cartilage tissue (*15*). To explore the role of Sirt5 in high-fat diet (HFD)-induced osteoarthritis (OA) development, we subjected both WT and *Sirt5*$^{-/-}$ mice to 20 weeks of either HFD or low-fat diet (LFD) to induce obesity. Prior to dietary intervention, female *Sirt5*$^{-/-}$ mice exhibited lower body weight compared to female WT mice, a distinction maintained under LFD conditions but gradually diminishing under HFD (Figure 2A, left panel). Similar weight disparities were observed in males pre-diet and with LFD, though HFD induced less weight gain in *Sirt5*$^{-/-}$ mice compared to WT (Figure 2B). Notably, despite lesser weight gain, *Sirt5*$^{-/-}$ mice displayed greater glucose intolerance than WT counterparts irrespective of sex (Figure 2C and 2D), indicative of systemic metabolic dysfunctions associated with Sirt5 deficiency. Furthermore, analysis of body composition revealed that HFD resulted in reduced lean mass percentage in both WT and *Sirt5*$^{-/-}$ mice across sexes. Interestingly, HFD led to increased fat mass specifically in female *Sirt5*$^{-/-}$ mice, whereas both male WT and *Sirt5*$^{-/-}$ mice showed elevated fat mass under HFD conditions (Figure 2E). These findings underscore the complex interplay between Sirt5 and metabolic homeostasis, highlighting Sirt5 as a potential modulator of diet-induced metabolic changes.

Next, we evaluated the knee joints of these mice. Under LFD conditions, *Sirt5*$^{-/-}$ mice exhibited early signs of proteoglycan loss compared to WT mice (Figure 3A, left panel). With HFD treatment, WT mice showed mild to moderate cartilage degeneration with superficial lesions across the joint surface, whereas *Sirt5*$^{-/-}$ mice displayed deeper and larger cartilage defects (Figure

3A, right panel). While no statistically significant differences were observed in OARSI scores among the groups (Figure 3B and 3I), male *Sirt5*$^{-/-}$ mice notably exhibited higher Mankin scores compared to their WT counterparts (Figure 3C and 3J). HFD exacerbated these differences more prominently in males than females (Figure 3C and 3J). Conversely, no significant differences were detected in osteophyte scores (Figure 3D and 3K) or Tidemark duplication scores (Figure 3F and 3M) between genotypes or sexes. *Sirt5*$^{-/-}$ mice also exhibited significantly higher cartilage damage scores, particularly exacerbated by HFD in males (Figure 3E and 3L). Regarding Safranin-O staining, female *Sirt5*$^{-/-}$ mice showed more than twice the loss of staining intensity of WT mice in both LFD and HFD groups (Figure 3G). In males, significant differences were observed only under HFD conditions (Figure 3N). Interestingly, hypertrophic chondrocytes were more prevalent in *Sirt5*$^{-/-}$ mice under both LFD and HFD conditions, particularly pronounced in males (Figure 3H and 3O). These findings underscore the differential impact of Sirt5 deficiency on cartilage integrity and osteoarthritis progression, influenced by diet and gender-specific factors.

Sirt5 cartilage specific knockout (*Sirt5-CKO*) does not affect systemic metabolism but promotes HFD induced OA development in mice in a sex-dependent manner

To elucidate the specific role of Sirt5 in joint-specific osteoarthritis (OA) development, we utilized *Aggrecan-Cre*^{ERT2} mice crossed with *Sirt5*$^{flox/flox}$ mice to achieve cartilage-specific knockout of Sirt5. Similarly, both wild-type (WT; *Sirt5*$^{flox/flox}$) and *Sirt5* conditional knockout (*Sirt5-CKO; Aggrecan-Cre*^{ERT2}*;Sirt5*$^{flox/flox}$) mice were administered Tamoxifen to induce *Sirt5* deletion, followed by exposure to either a HFD or LFD to induce obesity. Unlike systemic knockout models, WT and *Sirt5-CKO* mice showed similar weight gain under HFD conditions in both males and females (Figure 4A and 4B). Additionally, both groups exhibited comparable glucose intolerance following HFD treatment, as evidenced by nearly twofold increases in the area under the curve (AUC) during the intraperitoneal glucose tolerance test (ipGTT) compared to LFD groups, irrespective of sex (Figure 4C and 4D). Furthermore, HFD led to a reduction in lean mass in both WT and *Sirt5-CKO* mice regardless of sex (Figure 4E). Interestingly, only WT female mice, but not *Sirt5-CKO* females, showed a significantly higher percentage of fat mass under HFD conditions, possibly due to greater variability in fat accumulation among *Sirt5-CKO* mice. Conversely, in males, both WT and *Sirt5-CKO* mice exhibited significantly increased fat mass percentages after HFD exposure (Figure 4F). These findings highlight the joint-specific

implications of Sirt5 in metabolic responses to diet-induced obesity, independent of its effects on systemic metabolism.

We then investigated the role of cartilage-specific Sirt5 knockout in osteoarthritis (OA) development. Initially, we confirmed efficient deletion of Sirt5 specifically in cartilage, with no impact on other tissues such as muscle (Figure 5A). Subsequent joint analysis revealed that HFD induced typical moderate superficial cartilage lesions, proteoglycan loss, and osteophyte formation in WT mice (Figure 5B). In contrast, *Sirt5-CKO* mice subjected to HFD exhibited more extensive cartilage defects covering approximately half to two-thirds of the articular surface, along with pronounced osteophyte development at the medial tibial side (Figure 5B). Similar to findings from systemic knockout studies, OARSI scores did not show statistically significant differences between groups (Figure 5C and 5K). However, under HFD conditions, *Sirt5-CKO* males displayed significantly higher Mankin scores compared to WT mice, indicative of more severe OA in *Sirt5-CKO* mice (Figure 5D and 5L), consistent with histological observations (Figure 5B). While no statistical significance was observed for osteophyte scores (Figure 5E and 5M), *Sirt5-CKO* mice exhibited higher scores, suggesting a trend towards increased osteophyte formation compared to WT. Additionally, *Sirt5-CKO* males showed higher cartilage damage scores under HFD conditions, with no differences in tidemark duplication or hypertrophic chondrocyte scores observed in either sex (Figure 5G, 5I, 5O, and 5Q). In terms of proteoglycan staining, *Sirt5-CKO* males exhibited reduced staining compared to WT males (Figure 5H and 5N).

Furthermore, we conducted a knee hyperalgesia assay using pressure application measurement (PAM) to assess joint pain. Interestingly, we observed no significant changes in knee withdrawal thresholds among female mice across different groups (Figure 5J). In contrast, *Sirt5-CKO* males under HFD conditions showed a significant reduction in knee withdrawal threshold compared to LFD, suggesting increased susceptibility to knee hyperalgesia in *Sirt5-CKO* males under obesity conditions compared to WT (Figure 5R). These results highlight the specific impact of cartilage-specific Sirt5 deficiency on OA progression and pain sensitivity in a sex-dependent manner.

Sirt5 deficiency in chondrocytes results in decreased expression of extracellular matrix (ECM) proteins and increased expression of proinflammatory proteins

To investigate the role of Sirt5 deficiency in chondrocyte functions, we used proteomics to profile global protein expressions in WT and *Sirt5*$^{-/-}$ chondrocytes. Principle component analysis (PCA)

showed a non-overlapping distribution of WT and *Sirt5*$^{-/-}$ samples with 70.7% of the variation can be explained by the principle component 1 (genotype) (Figure 6A), suggesting distinct proteomic profiles of WT and *Sirt5*$^{-/-}$ chondrocytes. Furthermore, differential abundance analysis further highlighted significant alterations, revealing 520 upregulated and 566 downregulated proteins in *Sirt5*$^{-/-}$ chondrocytes compared to WT (Figure 6B). Notably, key extracellular matrix (ECM) proteins like COL2a1 and COL11a2 were markedly downregulated, whereas inflammation-associated mediators such as prostaglandin endoperoxide synthase 1 (PTGS1) and 15-hydroxyprostaglandin dehydrogenase (HPGD) were prominently upregulated in *Sirt5*$^{-/-}$ chondrocytes (Figure 6B). To delve deeper into these changes, we performed cluster analyses using the Online Search Tool for Retrieval of Interacting Genes/Proteins (STRING). The upregulated proteins indicated involvement in crucial signaling pathways such as the MAPK cascade, integrin-mediated signaling, and actin cytoskeleton organization. Conversely, the downregulated proteins were associated with metabolic pathways and collagen formation/cartilage development processes (Figure 6C). These findings align with the established roles of Sirt5 in cellular metabolism and strongly support our hypothesis that Sirt5 plays a pivotal role in cartilage tissue homeostasis and potentially in the development of osteoarthritis (OA).

Sirt5 regulated MaK is mainly targeting metabolic enzymes in chondrocytes

Our previous studies have demonstrated that Sirt5 plays a crucial role in regulating chondrocyte cellular metabolism and the post-translational modification of lysine residues through malonylation (*15*). To investigate the extent of malonylation in primary chondrocytes from WT and *Sirt5*$^{-/-}$ mice, we employed a previously established workflow for antibody-based enrichment and identification of peptides from protein digests containing malonylation modifications (MaK) (Figure 7A). In total, we quantified over 1,000 malonylated peptides covering 469 protein sites across all samples. Among these sites, 152 exhibited a measurable difference between WT and *Sirt5*$^{-/-}$ chondrocytes. Notably, 52.3% of the identified proteins had a single malonylation site, while 47.7% had two or more MaK sites (Figure 7B).

We performed KEGG pathway enrichment analysis on the malonylated proteins and found significant enrichment in pathways related to carbon metabolism and glycolysis/gluconeogenesis (Figure 7C). Glycolysis is a fundamental metabolic pathway in chondrocytes, providing ATP, and

our findings suggest that Sirt5-regulated malonylation targets key metabolic proteins in this context.

Given the enrichment of MaK modifications in glycolytic enzymes and the critical role of glycolysis in chondrocyte energy metabolism, we compared the relative abundance of MaK in all detected glycolytic enzymes between *Sirt5*$^{-/-}$ and WT chondrocytes. Among them, Glyceraldehyde 3-phosphate dehydrogenase (GAPDH), which catalyzes the conversion of glyceraldehyde 3-phosphate to glycerate 1,3-bisphosphate, showed significant dynamic regulation (with *Sirt5*$^{-/-}$/WT ratios of 3.1, 22.7, and -3.1 for three lysine sites) (Figure 7D).

To explore the functional implications of malonylation on these glycolytic enzymes and their regulation by Sirt5, we investigated whether modification of the most malonylated lysine 184 affects GAPDH enzymatic activity. We generated a mutated mouse GAPDH expression vector in which lysine 184 was substituted with glutamate (K184E), mimicking MaK modification by introducing a negatively charged residue. Mouse primary chondrocytes were transfected with either WT or mutant GAPDH. A kinetic enzymatic assay revealed that the GAPDH K184E mutant significantly reduced enzymatic reaction rates compared to both WT GAPDH and non-transfected controls (Figure 7E, 7F, and 7G). Furthermore, we measured the final glycolysis product lactate and found that the GAPDH K184E mutant also significantly decreased lactate production compared to WT GAPDH and control groups (Figure 7G). These results underscore the functional impact of Sirt5-regulated malonylation on glycolytic enzymes in chondrocytes, highlighting a novel regulatory mechanism in cellular metabolism.

Identification and functional analysis of a human OA-associated *SIRT5*^{F101L} mutation

We further explored the clinical relevance of our study. Using the Utah Population Database (UPDB), we identified families in which osteoarthritis (OA) segregates as a dominant trait, with multiple members diagnosed with early-onset or severe OA in various joints, including the 1st metatarsophalangeal joint, erosive hand OA, finger interphalangeal joint OA, thumb OA, or shoulder OA (*16-18*). We completed genomic analyses for 151 families and identified a rare *SIRT5* coding mutation (rs201979175, c.C303G:p.F101L, minor allele frequency - 0.00004303) in one family that segregates dominantly with finger interphalangeal joint OA (hand OA). Members of this family also have OA in other joints, including the spine, wrist, and shoulder (Figure 8A). The *SIRT5*^{F101L} mutation occurs in an evolutionarily conserved amino acid; the wild-type allele,

phenylalanine (F), is invariant in the vertebrate lineage (Figure 8B). The F101L mutation is located in the substrate binding domain (Figure 8B) and is predicted to be damaging or disease-causing by multiple in silico pathogenicity prediction programs (e.g., SIFT, MutationTaster). These data indicate that a rare, dominant coding mutation in *SIRT5* is associated with familial OA.

To determine if the *Sirt5*^{F101L} mutation alters Sirt5 protein function, we tested if overexpression of *Sirt5*^{F101L} in primary mouse chondrocytes affected protein MaK and gene expression. Primary mouse *Sirt5*$^{-/-}$ chondrocytes were transfected with WT or *Sirt5*^{F101L} and protein extracts were collected for MaK analysis. Immunoblot analysis indicates chondrocytes transfected with *Sirt5*^{F101L} have a higher level of MaK compared with WT (Figure 8C and 8D). WT and *Sirt5*^{F101L} transfected primary chondrocytes were also used for bulk RNA-seq analysis. Expression of *Sirt5*^{F101L} caused a reduction of multiple cartilage ECM genes (*Col11a2, Col9a1, Acan,* and *Col2a1*) and an increase of inflammation associated genes (*Nos2, Il6,* and *Vcam1*) (Figure 8F). These data are consistent with changes we observe in MaK levels and protein expression in *Sirt5*$^{-/-}$ chondrocytes (Figure 2B), suggesting that *Sirt5*^{F101L} is hypomorphic. In sum, our molecular, cellular and genetic data support a central role for SIRT5 in maintaining chondrocytes homeostasis.

DISCUSSION

Our study delves into the role of Sirtuin 5 (SIRT5) and its associated post-translational lysine malonylation in chondrocyte metabolism and osteoarthritis (OA) pathogenesis. We observed that aging and obesity lead to significant alterations in the expression and activity of SIRT5, contributing to cartilage degeneration and OA development. Our findings underscore the potential of targeting SIRT5 and its regulatory pathways as a therapeutic strategy for OA.

The sirtuin family of HDACs has seven highly conserved NAD-dependent deacetylases, which were discovered in 1999/2000 (*19, 20*). Sirtuins regulate key biological processes in mammals, including many aspects of metabolism, stress response, and signaling (*21*). In addition to their well-studied roles as lysine deacetylases, certain sirtuins can also remove other types of acyl modifications from lysine residues, including propionyl, butyryl, malonyl, succinyl, and the long-chain fatty-acid-derived myristoyl and palmitoyl groups (*9, 10, 22-24*). Sirtuins regulate numerous processes *in vivo*, including metabolism, DNA repair, metastasis, apoptosis, and translation, while promoting longevity and protecting against cancer (*21*). Sirt5 was initially reported as a lysine

deacetylase found in both mitochondria and cytoplasm (*25*). However, recent studies have shown it has low deacetylase activity and strong demalonylase and desuccinylase activity (*9*). Sirt5 deficiency in liver causes hypermalonylation of proteins that are enriched in glycolytic pathway, as identified by mass spectrometry of immunoprecipitated malonyl-lysine peptides (*11*). Consistently, *Sirt5*$^{-/-}$ hepatocytes show decreased production of lactic acid and reduced glycolytic flux (*11*). We previously reported that *Sirt5*$^{-/-}$ primary chondrocytes isolated *in vitro* have upregulated MaK and impaired cellular metabolism *(26)*. In this study, we further discovered that SIRT5 decreases in accordance with an increase of MaK during aging in both human and mouse cartilage. MaK has also been strongly implicated in the pathogenesis of metabolic diseases. For example, a large-scale analysis of protein malonylation in livers of *db/db* mice showed upregulated lysine malonylation of metabolic enzymes involved in glucose catabolism and FA oxidation (*27*). We also previously discovered that MaK level is increased in the cartilage of obese mice compared to lean mice (*8*). These early findings prompted us to further investigate the combined role of Sirt5 deficiency and obesity in OA development. Using both systemic and conditional knockout mouse models, our results demonstrated that obesity and Sirt5 deficiency synergistically promote chondrocyte metabolic dysfunction and cartilage degeneration. This finding potentially reveals a common signaling pathway through which aging and obesity—the two major risk factors for OA—converge to promote chondrocyte metabolic dysfunction and OA development.

Emerging evidence has suggested that acyl-based PTMs at lysine residues are crucial regulators of cellular metabolism. Proteomic studies identifying the malonylome, succinylome, and acetylome have found that metabolic proteins are enriched in these datasets (*10, 11*, *28-31*). Gene ontology analyses on acetylated proteins consistently reveal that metabolic pathways, including fatty acid metabolism, glycolysis, and amino acid metabolism, are among the top targets for these PTMs. However, it remains largely unknown how sites of malonylation, succinylation, and glutarylation identified in proteomic studies affect the activity of their targets and the pathophysiology at the whole-organismal level. Malonylation is a relatively unexplored PTM compared to succinylation and acetylation. Previous research has discovered that malonylation suppresses voltage-dependent anion channel 2 (VDAC2) (*32*), mTOR (*33*), glyceraldehyde 3-phosphate dehydrogenase (GAPDH) (*11*), while activating acetyl-coenzyme A (CoA) carboxylase 1 (ACC1) (*34*). Malonylation has been implicated in several pathophysiological processes, including sepsis-induced myocardial dysfunction (*32*), angiogenesis (*33*), and hepatic steatosis

(*34*). In this study, we are the first to use affinity enrichment-based proteomics to identify the malonylome in chondrocytes. We demonstrated a similar suppressive effect of GAPDH malonylation on its activity and glycolysis in chondrocytes. Combined with our data from both systemic and conditional Sirt5 knockout mouse models, our findings provide strong evidence that MaK in cartilage tissue during aging and obesity conditions could be an important underlying molecular mechanism for osteoarthritis (OA) development.

Our study provides significant insights into the sex-dependent effects of Sirt5 deficiency and HFD treatment on obesity and osteoarthritis (OA) development in mice. We found that systemic Sirt5 knockout (*Sirt5*$^{-/-}$) female mice maintained a lower body weight than wild-type (WT) under LFD, a difference that diminished with HFD. In males, *Sirt5*$^{-/-}$ mice gained less weight than WT under HFD, indicating that Sirt5 deficiency may mitigate some HFD-induced weight gain, especially in males. Despite lesser weight gain, both male and female *Sirt5*$^{-/-}$ mice showed greater glucose intolerance compared to WT controls, highlighting metabolic dysfunctions linked to Sirt5 deficiency. Interestingly, HFD increased fat mass specifically in female *Sirt5*$^{-/-}$ mice, while both male WT and *Sirt5*$^{-/-}$ mice had elevated fat mass. This suggests that female *Sirt5*$^{-/-}$ mice may be more susceptible to HFD-induced adiposity despite their lower body weight. These findings differ from a previous study showing no significant metabolic abnormalities in *Sirt5*$^{-/-}$ mice under either diet (*35*), possibly due to different HFD treatment durations (10 vs. 20 weeks). The systemic metabolic differences between WT and *Sirt5*$^{-/-}$ were not seen in the Sirt5-CKO study. These findings underscore the importance of considering sex as a biological variable in metabolic studies and suggest potential sex-specific mechanisms by which Sirt5 influences adiposity and glucose metabolism.

Interestingly, our results showed that male *Sirt5*$^{-/-}$ mice had higher Mankin scores and more cartilage damage under HFD conditions than females. Similarly, *Sirt5-CKO* mice under HFD had more cartilage defects and higher Mankin scores compared to WT mice, with males showing more severe OA. The pressure application measurement (PAM) assay demonstrated sex-dependent differences in OA pain. While knee withdrawal thresholds did not change significantly in female mice across groups, male *Sirt5-CKO* mice under HFD had a significant reduction in knee withdrawal threshold compared to LFD. These findings indicate a greater susceptibility to diet-induced OA progression in males and a potential sex-specific response to Sirt5 deficiency in joint tissues. Our results are consistent with well documented sex dependent differences of obesity and

OA pathogenesis in both clinical (*36, 37*) and preclinical studies. For example, it was found that male mice seem developing more consistent OA pathologies in response to different risk factors such as joint injury (*38, 39*) and aging (*40*). Since C57BL/6J female mice are typically more resistant to the obesogenic effects of a HFD treatment (*41, 42*), they are often excluded from obesity associated OA studies (*43*). Our results, to the best of our knowledge, are the first to report that, similar to joint injury-induced OA, obesity-associated OA appears to be more severe in males compared to females.

The identification of the human *SIRT5*^{F101L} mutation in a family with dominantly inherited osteoarthritis (OA) provides valuable insights into the genetic underpinnings of OA and underscores the critical role of SIRT5 in joint health. Our findings suggest that this rare mutation may reduce SIRT5 functions and contribute to the pathogenesis of OA through alterations in chondrocyte metabolism. The *SIRT5*^{F101L} mutation was identified in a multigenerational family with a high incidence of OA, affecting various joints, including the spine, wrist, and shoulder. The evolutionary conservation of the phenylalanine residue at position 101 and its predicted pathogenicity by multiple in silico tools strongly indicate the functional importance of this amino acid. The mutation's location in the substrate-binding domain suggests a potential impact on SIRT5's enzymatic activity, further supported by our functional assays demonstrating *Sirt5*^{F101L} has decreased demalonylase activity and disrupts gene expression in chondrocytes. Many (if not all) of the previously identified OA-associated mutations are non-null, even those identified from family studies (*44-50*). By studying a hypomorphic human OA-associated allele of *Sirt5*^{F101L}, we could potentially uncover novel metabolic and posttranslational effects that we could not detect using a null allele of *Sirt5*. Our on-going effort includes creating a novel mouse model harboring the *Sirt5*^{F101L} mutation and examine its susceptibility to different OA risk factors and identify potential chemical modulators to increase its enzymatic activity.

Our study also is not without limitations. Firstly, the mild osteoarthritis phenotype observed in mice during aging and obesity may not fully capture the complexity of the disease's progression in more severe cases. Additionally, the use of proteomics in *in vitro* cell culture may not accurately reflect the *in vivo* environment, potentially affecting the translatability of the results. Lastly, while the data we generated using cells transfected with *Sirt5*^{F101L} mutant provides valuable insights, they may not entirely replicate the physiological conditions *in vivo*. Therefore, more research directly

in the *Sirt5*^{F101L} mutant mice is needed to understand the mutation's role in osteoarthritis development.

In conclusion, our study has elucidated the critical role of Sirt5 and lysine malonylation (MaK) in chondrocyte metabolism and the pathogenesis of osteoarthritis (OA) during aging and obesity. We have demonstrated that Sirt5 deficiency, combined with obesity, significantly exacerbates joint degeneration in mice, and that MaK predominantly impacts metabolic pathways such as carbon metabolism and glycolysis. Furthermore, the discovery of a rare coding mutation in SIRT5 that segregates in a family with hand OA highlights the potential genetic contributions to OA development. These findings suggest that dysregulation of the Sirt5-MaK axis could be a pivotal mechanism underlying OA development associated with aging and obesity, offering new avenues for therapeutic interventions.

Acknowledgements

We thank the following funding support: Hevolution Foundation AGE award AGE-008 (SZ, HL), National Institutes of Health grant R01AR081804 (SZ, HL), National Institutes of Health grant R15AR080813 (SZ, HL), Arthritis National Research Foundation, The Arthritis & Aging Grant Program (SZ), American Society for Bone and Mineral Research FIRST award (SZ), Rheumatology Research Foundation Innovative Award (SZ), Osteopathic Heritage Foundation Ralph S. Licklider, D.O. Endowed Professorship (SZ), National Institutes of Health grant R01AR082973 (MJJ), Skaggs Foundation for Research (MJJ). We thank the staff (including Tammy Mace, Angela Smith, Shawn Rosensteel, and Scott Carpenter) at the animal facility in the Life Science Building for their excellent care for our animals. We thank Daniella Issa for her contributions to the *Sirt5*$^{-/-}$ mouse colony maintenance and Shadi Moradi for her help with the tissue dissections. We acknowledge the support of instrumentation for the Orbitrap Eclipse Tribrid system from the NCRR shared instrumentation grant 1S10 OD028654 (PI: Birgit Schilling). We thank the Chicago Center on Musculoskeletal Pain (funded by NIAMS P30AR079206, PI: Anne-Marie Malfait and Rachel E. Miller) for their training on using PAM to measure knee hyperalgesia in mice.

References

1. I. J. Wallace *et al.*, Knee osteoarthritis has doubled in prevalence since the mid-20th century. *Proc Natl Acad Sci U S A* **114**, 9332-9336 (2017).
2. E. Yelin, S. Weinstein, T. King, The burden of musculoskeletal diseases in the United States. *Semin Arthritis Rheum* **46**, 259-260 (2016).
3. A. Batushansky *et al.*, Fundamentals of OA. An initiative of Osteoarthritis and Cartilage. Obesity and metabolic factors in OA. *Osteoarthritis Cartilage* **30**, 501-515 (2022).
4. C. Carrico, J. G. Meyer, W. He, B. W. Gibson, E. Verdin, The Mitochondrial Acylome Emerges: Proteomics, Regulation by Sirtuins, and Metabolic and Disease Implications. *Cell Metab* **27**, 497-512 (2018).
5. A. G. Trub, M. D. Hirschey, Reactive Acyl-CoA Species Modify Proteins and Induce Carbon Stress. *Trends Biochem Sci* **43**, 369-379 (2018).
6. G. R. Wagner, M. D. Hirschey, Nonenzymatic protein acylation as a carbon stress regulated by sirtuin deacylases. *Mol Cell* **54**, 5-16 (2014).
7. M. D. Hirschey *et al.*, SIRT3 deficiency and mitochondrial protein hyperacetylation accelerate the development of the metabolic syndrome. *Mol Cell* **44**, 177-190 (2011).
8. H. Liu *et al.*, Cellular carbon stress is a mediator of obesity-associated osteoarthritis development. *Osteoarthritis Cartilage* **29**, 1346-1350 (2021).
9. J. Du *et al.*, Sirt5 is a NAD-dependent protein lysine demalonylase and desuccinylase. *Science* **334**, 806-809 (2011).
10. M. Tan *et al.*, Lysine glutarylation is a protein posttranslational modification regulated by SIRT5. *Cell Metab* **19**, 605-617 (2014).
11. Y. Nishida *et al.*, SIRT5 Regulates both Cytosolic and Mitochondrial Protein Malonylation with Glycolysis as a Major Target. *Mol Cell* **59**, 321-332 (2015).
12. J. M. Hollander, L. Zeng, The Emerging Role of Glucose Metabolism in Cartilage Development. *Curr Osteoporos Rep* **17**, 59-69 (2019).
13. R. Rajpurohit, K. Mansfield, K. Ohyama, D. Ewert, I. M. Shapiro, Chondrocyte death is linked to development of a mitochondrial membrane permeability transition in the growth plate. *J Cell Physiol* **179**, 287-296 (1999).
14. E. V. Tchetina, G. A. Markova, Regulation of energy metabolism in the growth plate and osteoarthritic chondrocytes. *Rheumatol Int* **38**, 1963-1974 (2018).

15. S. Zhu *et al.*, Sirt5 Deficiency Causes Posttranslational Protein Malonylation and Dysregulated Cellular Metabolism in Chondrocytes Under Obesity Conditions. *Cartilage* **13**, 1185S-1199S (2021).
16. C. M. Gavile *et al.*, Familial Clustering and Genetic Analysis of Severe Thumb Carpometacarpal Joint Osteoarthritis in a Large Statewide Cohort. *J Hand Surg Am* **47**, 923-933 (2022).
17. M. J. Jurynec *et al.*, NOD/RIPK2 signalling pathway contributes to osteoarthritis susceptibility. *Ann Rheum Dis* **81**, 1465-1473 (2022).
18. N. H. Kazmers *et al.*, Familial Clustering of Erosive Hand Osteoarthritis in a Large Statewide Cohort. *Arthritis Rheumatol* **73**, 440-447 (2021).
19. R. A. Frye, Characterization of five human cDNAs with homology to the yeast SIR2 gene: Sir2-like proteins (sirtuins) metabolize NAD and may have protein ADP-ribosyltransferase activity. *Biochem Biophys Res Commun* **260**, 273-279 (1999).
20. R. A. Frye, Phylogenetic classification of prokaryotic and eukaryotic Sir2-like proteins. *Biochem Biophys Res Commun* **273**, 793-798 (2000).
21. J. A. Hall, J. E. Dominy, Y. Lee, P. Puigserver, The sirtuin family's role in aging and age-associated pathologies. *J Clin Invest* **123**, 973-979 (2013).
22. S. Imai, C. M. Armstrong, M. Kaeberlein, L. Guarente, Transcriptional silencing and longevity protein Sir2 is an NAD-dependent histone deacetylase. *Nature* **403**, 795-800 (2000).
23. H. Jiang *et al.*, SIRT6 regulates TNF-alpha secretion through hydrolysis of long-chain fatty acyl lysine. *Nature* **496**, 110-113 (2013).
24. C. Peng *et al.*, The first identification of lysine malonylation substrates and its regulatory enzyme. *Mol Cell Proteomics* **10**, M111 012658 (2011).
25. U. Mahlknecht, A. D. Ho, S. Letzel, S. Voelter-Mahlknecht, Assignment of the NAD-dependent deacetylase sirtuin 5 gene (SIRT5) to human chromosome band 6p23 by in situ hybridization. *Cytogenet Genome Res* **112**, 208-212 (2006).
26. S. Zhu *et al.*, Sirt5 Deficiency Causes Posttranslational Protein Malonylation and Dysregulated Cellular Metabolism in Chondrocytes Under Obesity Conditions. *Cartilage*, 1947603521993209 (2021).

27. Y. Du *et al.*, Lysine malonylation is elevated in type 2 diabetic mouse models and enriched in metabolic associated proteins. *Mol Cell Proteomics* **14**, 227-236 (2015).
28. J. Park *et al.*, SIRT5-mediated lysine desuccinylation impacts diverse metabolic pathways. *Mol Cell* **50**, 919-930 (2013).
29. M. J. Rardin *et al.*, SIRT5 regulates the mitochondrial lysine succinylome and metabolic networks. *Cell Metab* **18**, 920-933 (2013).
30. B. T. Weinert *et al.*, Lysine succinylation is a frequently occurring modification in prokaryotes and eukaryotes and extensively overlaps with acetylation. *Cell Rep* **4**, 842-851 (2013).
31. M. J. Rardin *et al.*, Label-free quantitative proteomics of the lysine acetylome in mitochondria identifies substrates of SIRT3 in metabolic pathways. *Proc Natl Acad Sci U S A* **110**, 6601-6606 (2013).
32. H. She *et al.*, VDAC2 malonylation participates in sepsis-induced myocardial dysfunction via mitochondrial-related ferroptosis. *Int J Biol Sci* **19**, 3143-3158 (2023).
33. U. Bruning *et al.*, Impairment of Angiogenesis by Fatty Acid Synthase Inhibition Involves mTOR Malonylation. *Cell Metab* **28**, 866-880 e815 (2018).
34. H. Cao *et al.*, Malonylation of Acetyl-CoA carboxylase 1 promotes hepatic steatosis and is attenuated by ketogenic diet in NAFLD. *Cell Rep* **42**, 112319 (2023).
35. J. Yu *et al.*, Metabolic characterization of a Sirt5 deficient mouse model. *Sci Rep* **3**, 2806 (2013).
36. N. A. Segal, J. M. Nilges, W. M. Oo, Sex differences in osteoarthritis prevalence, pain perception, physical function and therapeutics. *Osteoarthritis Cartilage*, (2024).
37. M. Tschon, D. Contartese, S. Pagani, V. Borsari, M. Fini, Gender and Sex Are Key Determinants in Osteoarthritis Not Only Confounding Variables. A Systematic Review of Clinical Data. *J Clin Med* **10**, (2021).
38. H. S. Hwang, I. Y. Park, J. I. Hong, J. R. Kim, H. A. Kim, Comparison of joint degeneration and pain in male and female mice in DMM model of osteoarthritis. *Osteoarthritis Cartilage* **29**, 728-738 (2021).
39. R. K. Komaravolu *et al.*, Sex-specific effects of injury and beta-adrenergic activation on metabolic and inflammatory mediators in a murine model of post-traumatic osteoarthritis. *Osteoarthritis Cartilage*, (2024).

40. T. Geraghty *et al.*, Age-Associated Changes in Knee Osteoarthritis, Pain-Related Behaviors, and Dorsal Root Ganglia Immunophenotyping of Male and Female Mice. *Arthritis Rheumatol* **75**, 1770-1780 (2023).
41. I. Casimiro, N. D. Stull, S. A. Tersey, R. G. Mirmira, Phenotypic sexual dimorphism in response to dietary fat manipulation in C57BL/6J mice. *J Diabetes Complications* **35**, 107795 (2021).
42. R. R. Gelineau *et al.*, The behavioral and physiological effects of high-fat diet and alcohol consumption: Sex differences in C57BL6/J mice. *Brain Behav* **7**, e00708 (2017).
43. S. Zhu *et al.*, Sirt3 Promotes Chondrogenesis, Chondrocyte Mitochondrial Respiration and the Development of High-Fat Diet-Induced Osteoarthritis in Mice. *J Bone Miner Res* **37**, 2531-2547 (2022).
44. G. Aubourg, S. J. Rice, P. Bruce-Wootton, J. Loughlin, Genetics of osteoarthritis. *Osteoarthritis Cartilage* **30**, 636-649 (2022).
45. C. G. Boer *et al.*, Deciphering osteoarthritis genetics across 826,690 individuals from 9 populations. *Cell* **184**, 4784-4818 e4717 (2021).
46. C. M. Gavile *et al.*, Familial Clustering and Genetic Analysis of Severe Thumb Carpometacarpal Joint Osteoarthritis in a Large Statewide Cohort. *J Hand Surg Am*, (2022).
47. M. J. Jurynec *et al.*, NOD/RIPK2 signalling pathway contributes to osteoarthritis susceptibility. *Ann Rheum Dis*, (2022).
48. M. J. Jurynec *et al.*, A hyperactivating proinflammatory RIPK2 allele associated with early-onset osteoarthritis. *Hum Mol Genet* **27**, 2406 (2018).
49. E. Sliz *et al.*, TUFT1, a novel candidate gene for metatarsophalangeal osteoarthritis, plays a role in chondrogenesis on a calcium-related pathway. *PLoS One* **12**, e0175474 (2017).
50. U. Styrkarsdottir *et al.*, Meta-analysis of erosive hand osteoarthritis identifies four common variants that associate with relatively large effect. *Ann Rheum Dis*, (2023).

Figure 1. Sirt5 decreases while MaK increases in cartilage during aging. (**A**) Immunohistochemical staining for SIRT5 and lysine malonylation (MaK) in the human articular cartilage tissues from young and old donors (n=3). Insert boxes show the magnified images of the dashed squared area. (**B**) Quantification of the ratio of strongly-, or weakly-, or non-stained

chondrocytes to total chondrocytes. (**C**) Immunoblotting for MaK and β-actin in the articular cartilage tissues from mice of different ages (25, 48, and 90 wks). (D) Quantification of the MaK relative to β-actin level (n=4). Data are expressed as the means ± SD, **P* < 0.05, ***P* < 0.01, and ****P* < 0.001 by Student's *t* test.

Figure 2. Sirt5 systemic knockout perturbs metabolism in mice. (**A**) Weight changes of *Sirt5*$^{-/-}$ and WT mice during a 20-week high-fat diet (HFD) or low-fat diet (LFD) feeding. Females (n=6 for the WT-LFD, n=7 for the WT-HFD, n=9 for the *Sirt5*$^{-/-}$-LFD, and n=9 for the *Sirt5*$^{-/-}$-HFD) are on the left and males (n=8 for the WT-LFD, n=9 for the WT-HFD, n=10 for the *Sirt5*$^{-/-}$-LFD, and n=10 for the *Sirt5*$^{-/-}$-HFD) are on the right. (**B**) Weight changes of *Sirt5*$^{-/-}$ and WT mice after the diet feeding. Females are on the left and males are on the right. (**C**) Intraperitoneal Glucose Tolerance Test (ipGTT) in female *Sirt5*$^{-/-}$ and WT mice after HFD or LFD diet feeding (left panel). The areas under the curve based on the ipGTT results are depicted in the right panel. (**D**) Intraperitoneal Glucose Tolerance Test (ipGTT) in male *Sirt5*$^{-/-}$ and WT mice after HFD or LFD diet feeding (left panel). The areas under the curve based on the ipGTT results are depicted in the right panel. (**E**) Lean mass of *Sirt5*$^{-/-}$ and WT mice after the diet feeding. Females are on the left and males are on the right. (**F**) Fat mass of *Sirt5*$^{-/-}$ and WT mice after the diet feeding. Females are on the left and males are on the right. Data are expressed as the means ± SD, **P* < 0.05, ***P* < 0.01, and ****P* < 0.001 by two-way ANOVA.

Figure 3. Sirt5 systemic knockout mice develop more severe HFD induced OA. (**A**) Fast Green/Safranin Orange staining of *Sirt5*$^{-/-}$ and WT mouse knee joints (28 weeks old). Pictures show the medial tibias. Asterix indicates loss of proteoglycan staining and superficial degeneration. Arrows indicate cartilage defects. (**B-H**) Quantifications of OA severity in female *Sirt5*$^{-/-}$ and WT mouse knee joints. The OA scores include OARSI (**B**), Mankin (**C**), Osteophyte (**D**), Cartilage damage (**E**), Tidemark duplication (**F**), Saf-O staining (**G**), and Hypertrophic chondrocytes (**H**). (**H-O**) Quantifications of OA severity in male *Sirt5*$^{-/-}$ and WT mouse knee joints. . Data are expressed as the means ± SD, **P* < 0.05, ***P* < 0.01, and ****P* < 0.001 by two-way ANOVA.

Figure 4. Sirt5 cartilage specific knockout (*Sirt5-CKO*) minimally perturbs metabolism in mice. (**A**) Weight changes of *Sirt5-CKO* and WT mice during a 24-week HFD or LFD feeding.

Females (n=6 for the WT-LFD, n=7 for the WT-HFD, n=9 for the *Sirt5*$^{-/-}$-LFD, and n=9 for the *Sirt5*$^{-/-}$-HFD) are on the left and males (n=13 for the WT-LFD, n=10 for the WT-HFD, n=14 for the *Sirt5*$^{-/-}$-LFD, and n=10 for the *Sirt5*$^{-/-}$-HFD) are on the right. (**B**) Weight changes of *Sirt5-CKO* and WT mice after the diet feeding. Females are on the left and males are on the right. (**C**) Intraperitoneal Glucose Tolerance Test (ipGTT) in female *Sirt5-CKO* and WT mice after HFD or LFD diet feeding (left panel). The areas under the curve based on the ipGTT results are depicted in the right panel. (**D**) Intraperitoneal Glucose Tolerance Test (ipGTT) in male *Sirt5-CKO* and WT mice after HFD or LFD diet feeding (left panel). The areas under the curve based on the ipGTT results are depicted in the right panel. (**E**) Lean mass of *Sirt5-CKO* and WT mice after the diet feeding. Females are on the left and males are on the right. (**F**) Fat mass of *Sirt5-CKO* and WT mice after the diet feeding. Females are on the left and males are on the right. Data are expressed as the means ± SD, **P* < 0.05, ***P* < 0.01, and ****P* < 0.001 by two-way ANOVA.

Figure 5. Sirt5 cartilage specific knockout mice (*Sirt5-CKO*) develop more severe HFD induced OA. (**A**) Western blotting for SIRT5 protein in both cartilage and muscle tissue in *Sirt5-CKO* and WT mice. (**B**) Fast Green/Safranin Orange staining of *Sirt5-CKO* and WT mouse knee joints (32 weeks old). Pictures show the medial compartments including both femur and tibia. (**C-I**) Quantifications of OA severity in female *Sirt5-CKO* and WT mouse knee joints. The OA scores include OARSI (**C**), Mankin (**D**), Osteophyte (**E**), Cartilage damage (**F**), Tidemark duplication (**G**), Saf-O staining (**H**), and Hypertrophic chondrocytes (**I**). (**J**) Knee hyperalgesia as an indicator for OA pain assessed in the same female mice. (**K-Q**) Quantifications of OA severity in male *Sirt5-CKO* and WT mouse knee joints. (**R**) Knee hyperalgesia as an indicator for OA pain assessed in the same male mice. Data are expressed as the means ± SD, **P* < 0.05, ***P* < 0.01, and ****P* < 0.001 by two-way ANOVA.

Figure 6. Sirt5 deficiency in chondrocytes results in decreased expression of extracellular proteins and increased expression of pro-inflammatory proteins. (**A**) Principal Component Analysis (PCA) plot of *Sirt5*$^{-/-}$ and WT mouse chondrocyte proteomic samples (n=3). (**B**) Volcano plot depicting protein differential regulation between *Sirt5*$^{-/-}$ vs. WT samples. Red and blue denote significant upregulation and significant downregulation, respectively. Top 10 upregulated/downregulated proteins as based on magnitude of log2 fold-change are labelled in-

plot. (**C**) Overview of protein interaction analysis. Given are all clusters of significantly upregulated/downregulated proteins that contain at least 10 proteins. Functional annotation summaries are representative based on enriched Gene Ontology biological process and Reactome pathway terms. Top hubs have been defined on eigenvector centrality. Accompanying heatmap depicts mean abundance Z-score of each cluster in each sample.

Figure 7. Enrichment and identification of lysine malonylome in mouse primary chondrocytes by label-free quantification. (**A**) Schematic description of experimental procedures of the label-free quantification of lysine malonylome. (**B**) Distribution of the number of MaK sites identified per protein in chondrocytes. Most malonylated proteins contain a single site, but some contain multiple sites. (**C**) KEGG pathway enrichment analysis of malonylated proteins in chondrocytes. Numbers in the brackets show the number of malonylated proteins in the pathways. (**D**) Sites of malonylation in the GAPDH protein with respect to its two functional domains, NAD binding, and catalytic domains. The ratio of malonylation between WT and *Sirt5*$^{-/-}$ samples are shown above. (**E**) GAPDH enzymatic activity kinetics assay. The assay includes on-transfected control (Ctrl), wild type GAPDH, and mutant GAPDH (K184E). (**F**) Western blotting for GAPDH to confirm successful transfection of WT and mutant GAPDH in chondrocytes. (**G**) Quantifications of GAPDH activity in mouse primary chondrocytes transfected with WT or mutant GAPDH. (**I**) Quantification of lactate production in mouse primary chondrocytes transfected with WT or mutant GAPDH. Data are expressed as the means ± SD, **P* < 0.05, ***P* < 0.01, and ****P* < 0.001 by T-test.

Figure 8. Identification of the human OA-associated *SIRT5*^{F101L} mutation. (**A**) A rare *SIRT5* coding mutation dominantly segregates in a family with hand OA. Circles = females, square = males, black circles/squares = individuals affected with hand OA and individuals also had other joints affected. (**B**) Whole exome sequencing identified a mutation in a highly conserved amino acid (F101L) (F is invariant in the vertebrate lineage) in the substrate binding domain of SIRT5. (**C**) Western blotting analysis indicates chondrocytes transfected with *SIRT5*^{F101L} mutant have a higher level of MaK comparing with WT. (**D**) Quantification of the band intensity between WT and *SIRT5*^{F101L} mutant in the blot in panel (C). (n=3) (**D**) Bulk RNA-Seq analysis of primary mouse chondrocytes transfected with WT or *SIRT5*^{F101L} mutant constructs. Expression of *Sirt5*^{F101L} causes

a reduction of multiple cartilage ECM genes (*Col11a2, Col9a1, Acan, and Col2a1*) and an increase of inflammation associated genes (*Nos2, Il6, and Vcam1*) (n=3). (**E**) List of upregulated or downregulated genes as colored in the panel (C). Asterix indicates statistically significantly changed genes, p values are shown above each gene. Data are expressed as the means ± SD, **P* < 0.05, ***P* < 0.01, and ****P* < 0.001 by T-test.

Figure 1

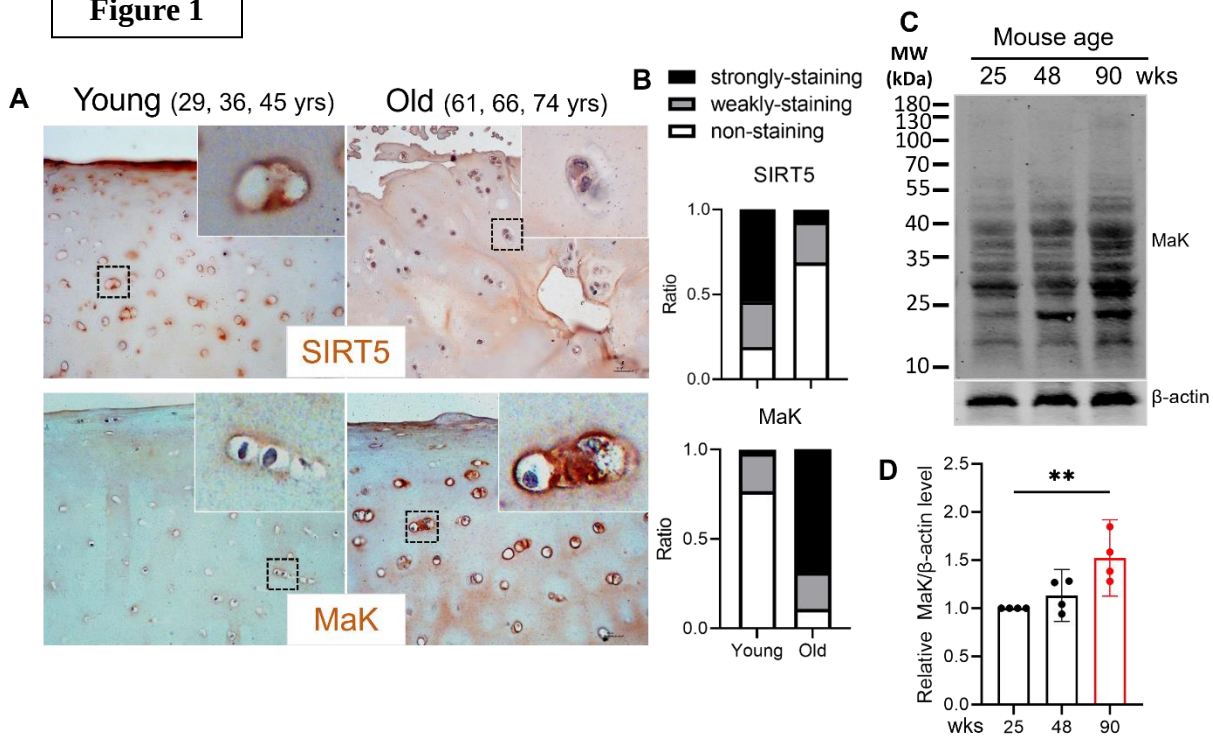

Figure 2

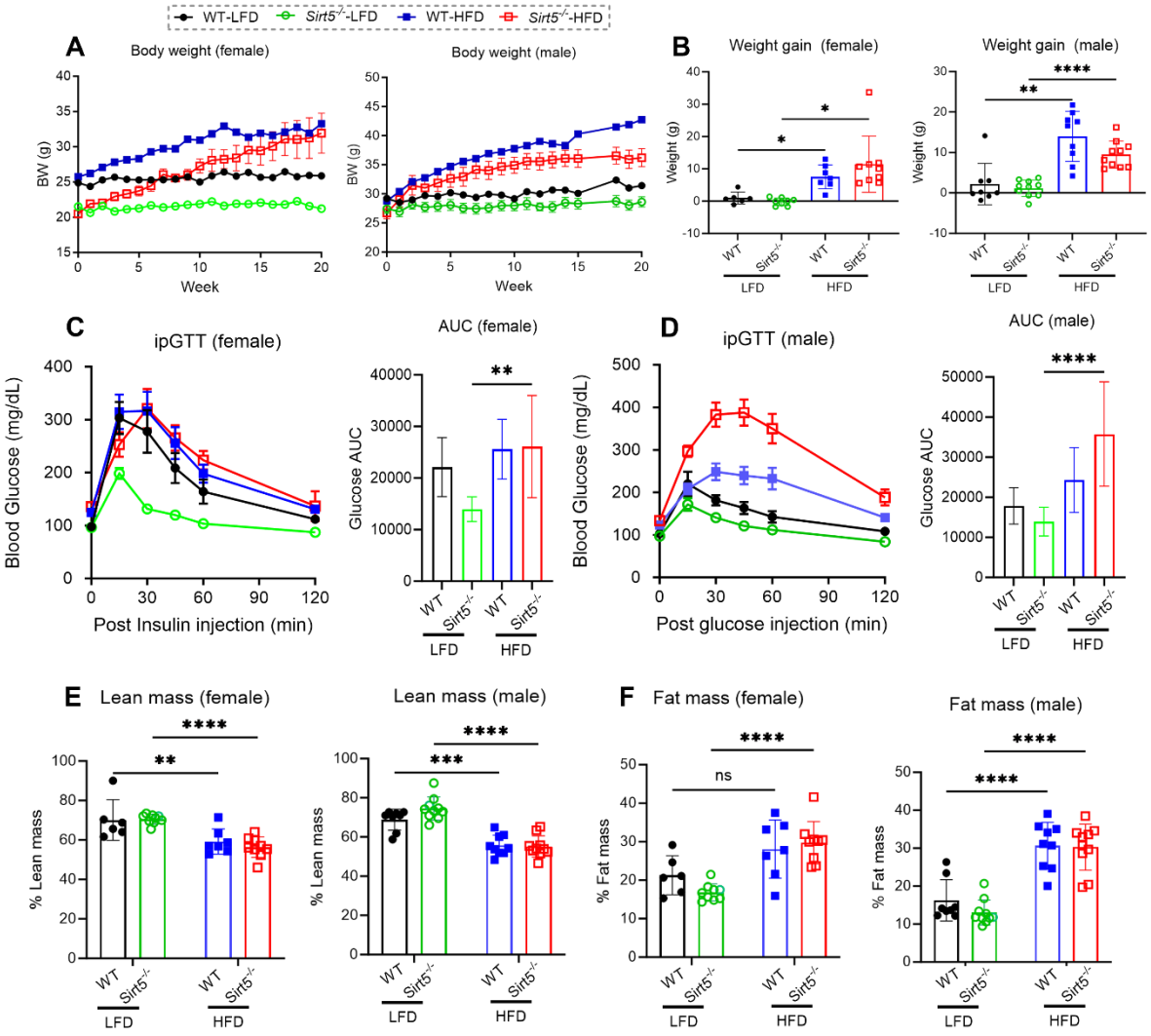

Figure 3

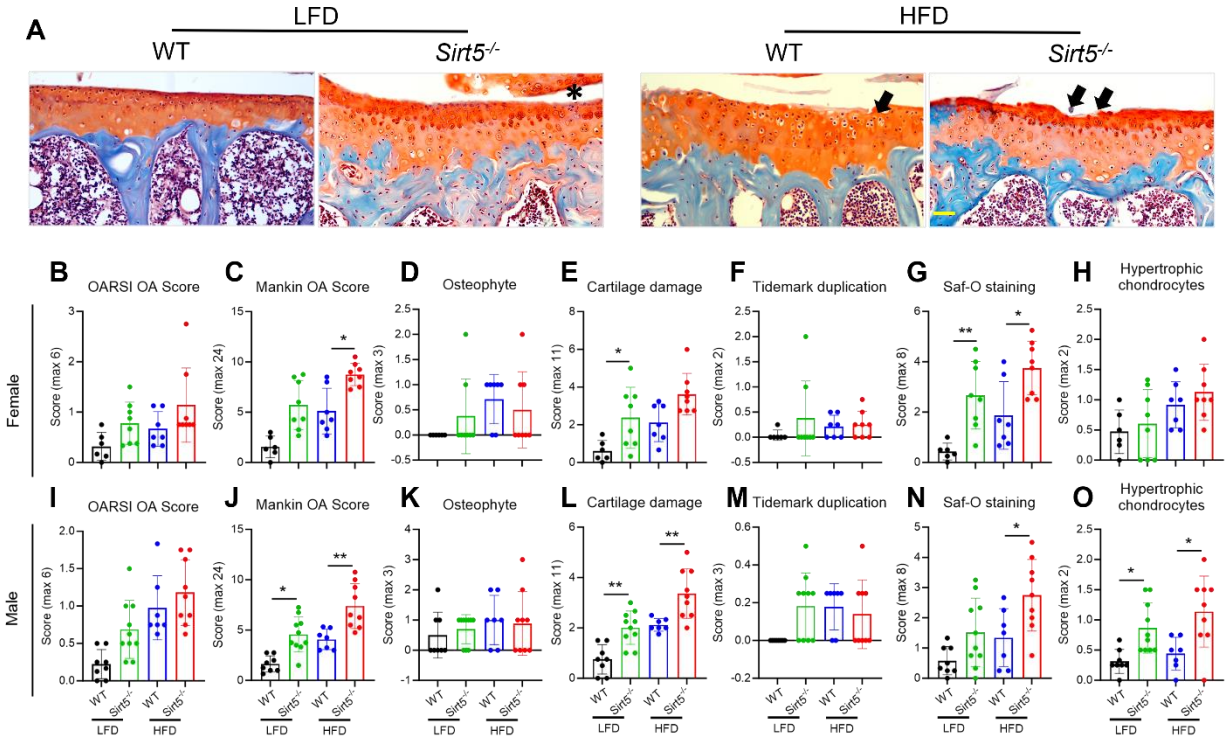

Figure 4

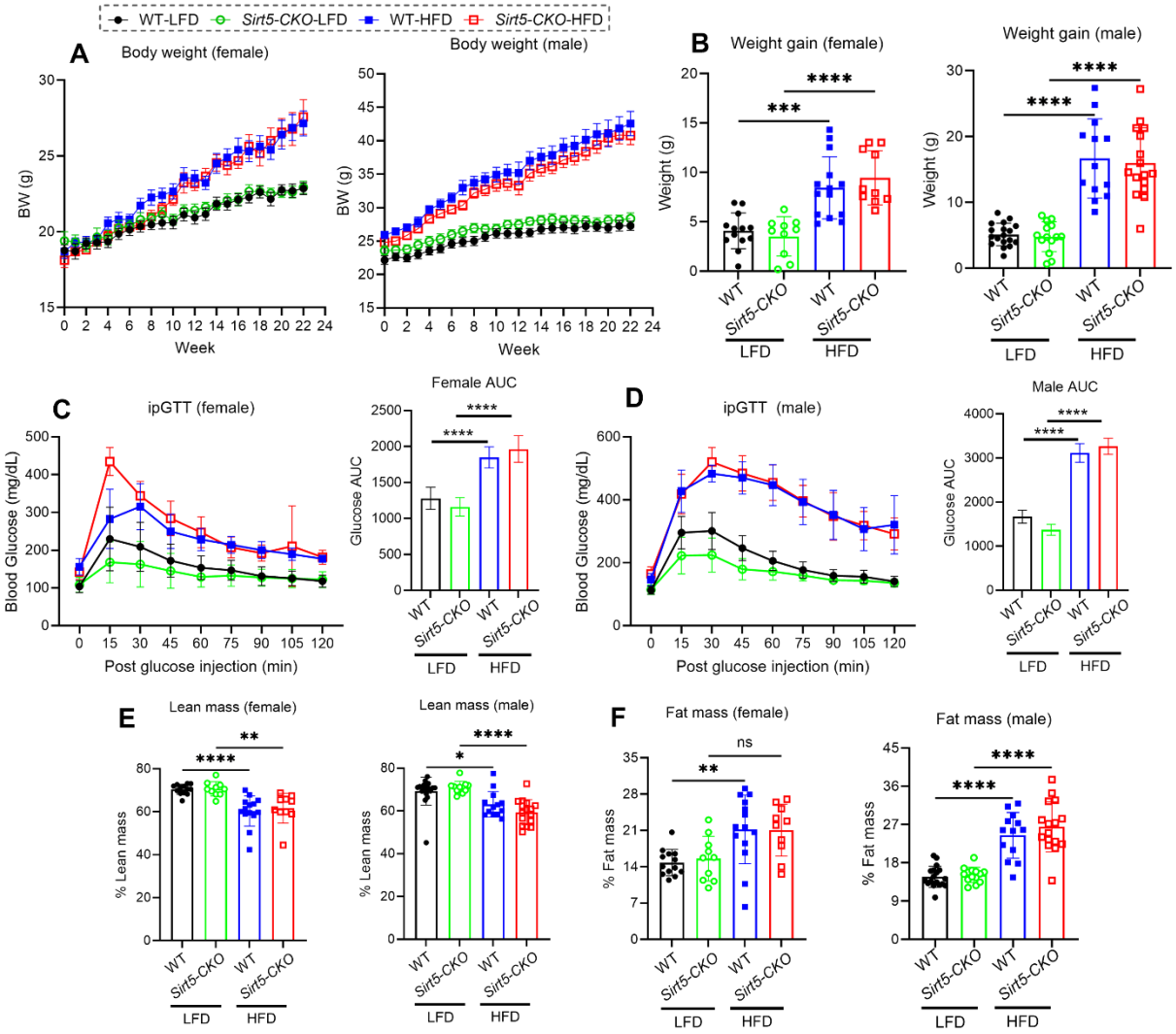

Figure 5

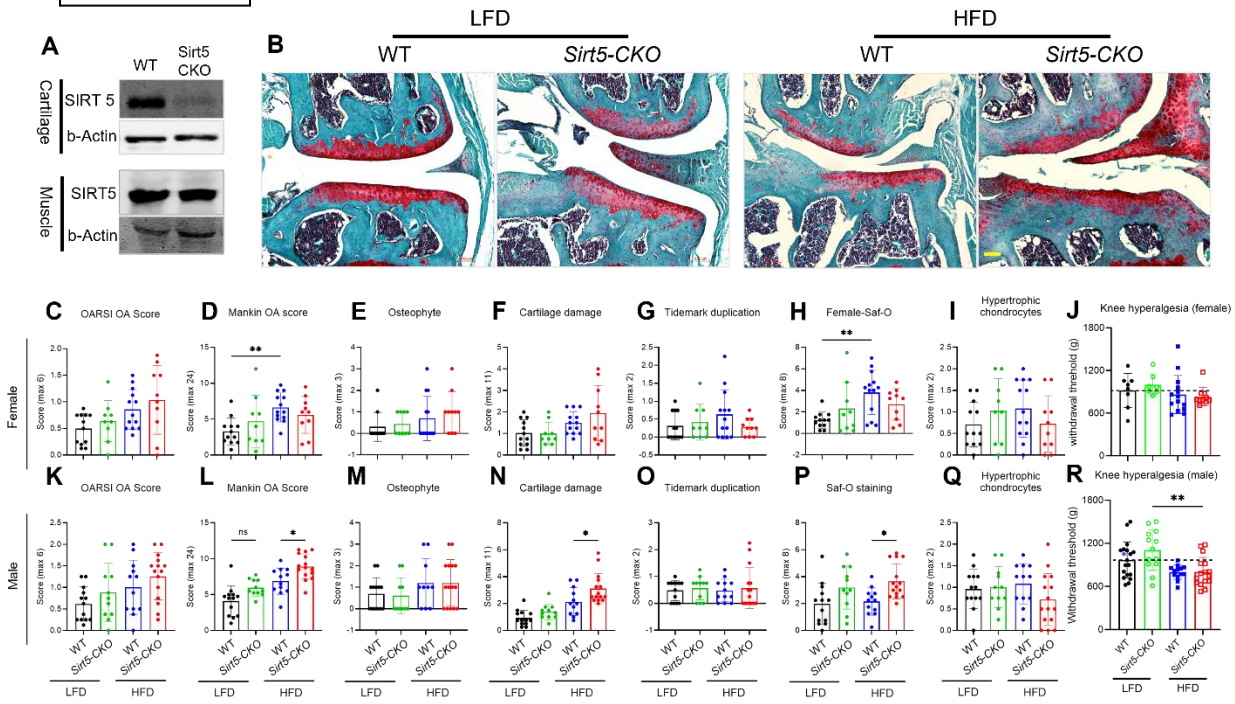

Figure 6

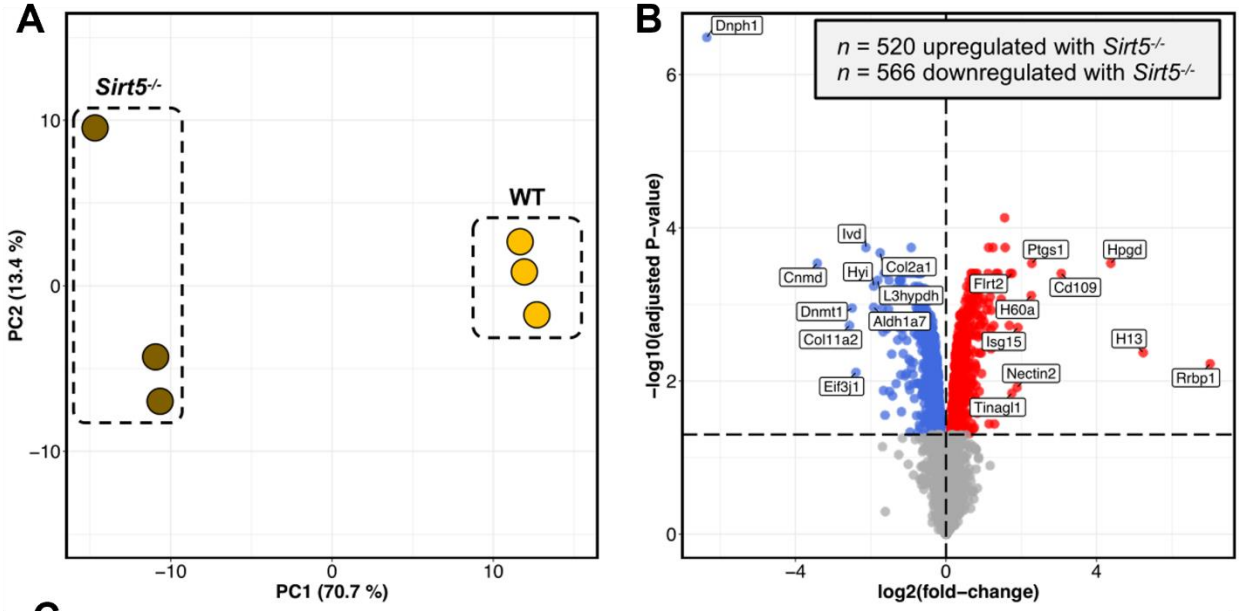

C

	Cluster ID	Size	Functional Annotation Summary	Top Hub
Upregulated proteins	UR C1	31	signal transduction / MAPK cascade / signaling by GPCR	Src
	UR C2	15	Arp2/3 complex-mediated actin nucleation	Arpc1b
	UR C3	14	integrin-mediated signaling pathway / cell adhesion	Itgb1
	UR C4	13	actin cytoskeleton organization	Vcl
	UR C5	11	vesicle-mediated transport / exocytosis / autophagy	Vps18
	UR C6	10	vesicle docking / exocytosis / cytokinesis / cell cycle / secretion	Exoc3
Downregulated proteins	DR C1	72	mRNA splicing / RNA splicing	Snrpd3
	DR C2	41	translation / metabolism of proteins	Rpl4
	DR C3	32	ribosome biogenesis / rRNA processing / metabolism of RNA	Nop56
	DR C4	25	cell cycle / chromosome organization / DNA replication	Mcm7
	DR C5	17	oxidative phosphorylation / mitochondrion organization	Ndufa5
	DR C6	13	collagen formation / cartilage tissue development	Pcolce
	DR C7	11	protein folding	Hsp90ab1
	DR C8	11	signal transduction / insulin receptor signaling pathway	Pik3r1
	DR C9	11	metabolism of lipids / metabolism of amino acids and derivatives	Acadm
	DR C10	10	metabolism of lipids	Acat1

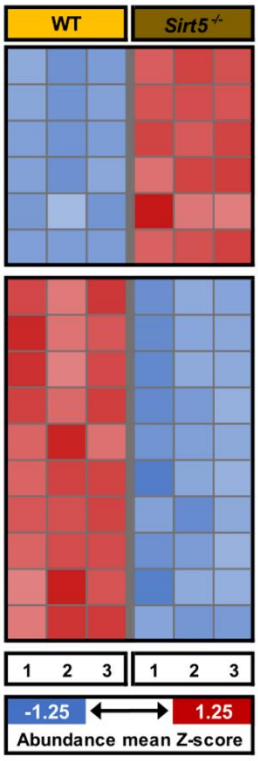

Figure 7

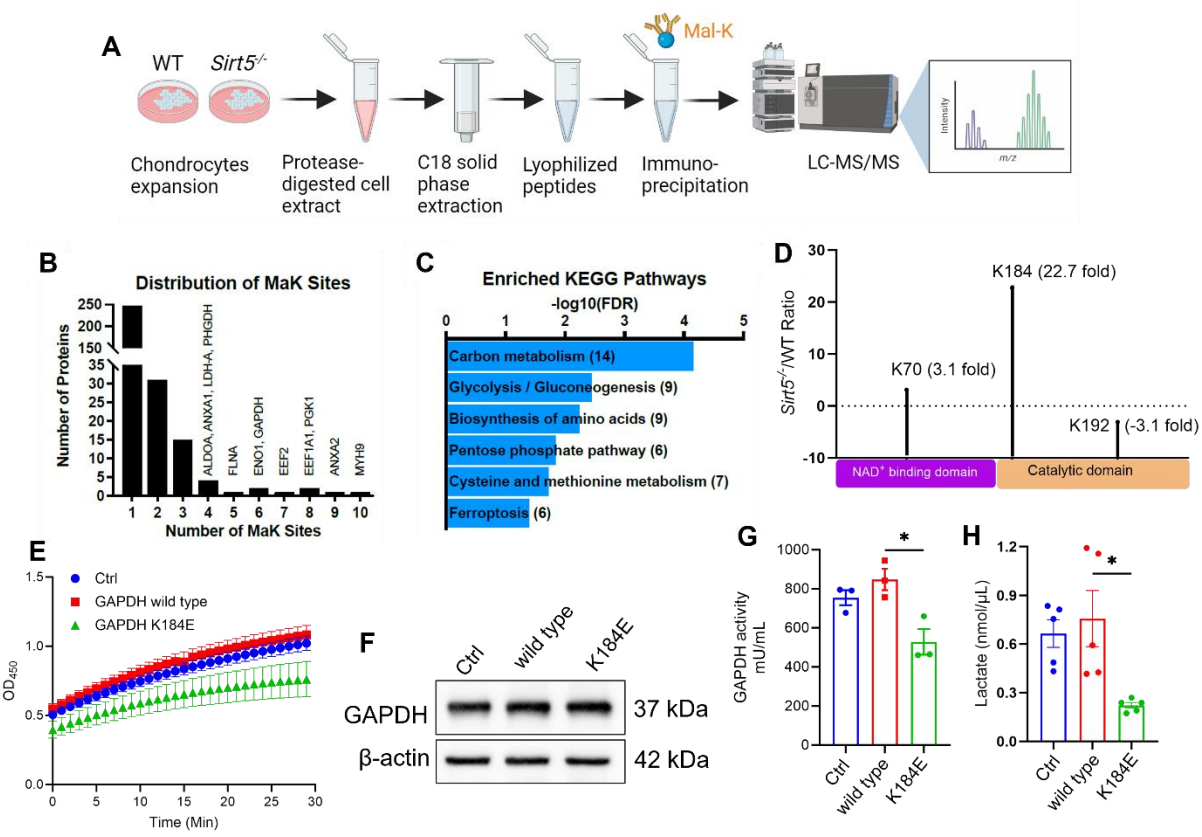

Figure 8